

# High-Affinity Antibody Detection with a Bivalent Circularized Peptide Containing Antibody-Binding Domains

Fangyu Zhou, Andrew Kroetsch, Vyncent P. Nguyen, Xiao Huang, Ogechi Ogoke, Natesh Parashurama, and Sheldon Park\*

Direct chemical labeling of antibody produces molecules with poorly defined modifications. Use of a small antibody-binding protein as an adapter can simplify antibody functionalization by forming a specific antibody-bound complex and introducing site-specific modifications. To stabilize a noncovalent antibody complex that may be used without chemical crosslinking, a bivalent antibody-binding protein is engineered with an improved affinity of interaction by joining two Z domains with a conformationally flexible linker. The linker is essential for the increase in affinity because it allows simultaneous binding of both domains. The molecule is further circularized using a split intein, creating a novel adapter protein ("lasso"), which binds human immunoglobulin G1 (IgG1) with  $K_D = 0.53$  nM and a dissociation rate that is 55- to 84-fold slower than Z. The lasso contains a unique cysteine for conjugation with a reporter and may be engineered to introduce other functional groups, including a biotin tag and protease recognition sequences. When used in enzyme-linked immunosorbent assay (ELISA), the lasso generates a stronger reporter signal compared to a secondary antibody and lowers the limit of detection by 12-fold. The small size of the lasso and a long half-life of dissociation make the peptide a useful tool in antibody detection and immobilization.

## 1. Introduction

Antibodies are widely used in medicine and research because of their ability to interact with their antigens with high affinity and

specificity.<sup>[1,2]</sup> Antibody-binding proteins have similarly found applications in biotechnology to facilitate the use of antibody-based technologies.<sup>[3,4]</sup> Of these, bacterial surface proteins from *Staphylococcus aureus* protein A (SpA), group C and G of streptococcal bacteria (protein G), and *Peptostreptococcus magnus* (protein L) are most often used,<sup>[5,6]</sup> while other less-utilized antibody-binding proteins also exist.<sup>[7,8]</sup> Since their discoveries, numerous biochemical and structural studies have sharpened our understanding of how these molecules interact with antibodies,<sup>[9–12]</sup> and their molecular properties have been repeatedly engineered to cater to varying needs that arise in different contexts.<sup>[13]</sup> The earliest examples of their use in biotechnology involve affinity purification using immobilized bacterial antibody-binding proteins (bABPs).<sup>[14–17]</sup> Affinity purification continues to be an important area of application for bABPs. Because a low pH treatment used to elute bound antibody may cause denaturation,<sup>[18–20]</sup> variants that allow dissociation of the bound antibody under milder elution

conditions have also been engineered.

Other applications of antibody-binding proteins require a different affinity profile. Unlike affinity purification, which must balance efficient antibody capture with facile elution, achieving the most stable and specific interaction is essential for detection and labeling. Known bABPs are multidomain proteins, which allow high-affinity interaction through multivalent binding. For example, SpA contains five homologous domains, each of which is capable of antibody binding<sup>[21]</sup> and has been used in enzyme-linked immunosorbent assay (ELISA)<sup>[22]</sup> and surface plasmon resonance (SPR).<sup>[23]</sup> However, it is difficult to produce full-length SpA in large quantities and forms poorly defined two-to-one antibody-to-SpA complexes when mixed with antibodies.<sup>[24]</sup> To simplify its construction and application, a single-domain variant, Z domain, with 58 amino acids has been engineered from the B domain of SpA and is often used in biotechnology.<sup>[25]</sup> The Z domain is small, resistant to aggregation, and binds certain antibody species and isotypes with high affinity.

One of the potential uses of single-antibody-binding domain (ABD) proteins, such as Z and C2 of protein G, is to introduce site-directed modifications to an antibody. Antibodies are often chemically biotinylated or conjugated with fluorophores, enzymes or drugs before use.<sup>[26–29]</sup> Covalent modifications can be introduced at primary amines (e.g., lysine and the amino

F. Zhou, A. Kroetsch, V. P. Nguyen, X. Huang, O. Ogoke, Prof. N. Parashurama, Prof. S. Park  
Department of Chemical and Biological Engineering  
University at Buffalo  
Buffalo, NY 14260, USA  
E-mail: sjpark6@buffalo.edu

Present address: HarkerBio, L.L.C., 700 Ellicott Street, Buffalo, NY 14203, USA

These authors have contributed equally.

Present address: Biologics Drug Product Development, Sanofi Research and Development, 5 The Mountain Rd. Framingham, MA

Present address: Albany Molecular Research Inc., 1001 Main Street, Buffalo, New York, NY 14203, USA

Present address: Genewiz Inc, 115 Corporate Blvd, South Plainfield, NJ 07080

DOI: 10.1002/biot.201800647

terminus), carboxyl groups (e.g., aspartic and glutamic acids), and thiols (cysteine) using established technologies,<sup>[30]</sup> but chemical conjugation does not allow precise control of the degree or location of modification. On the one hand, the degree of modification needs to be kept low to avoid potential loss of activity, which can occur if the residues important for antigen binding are accidentally modified.<sup>[31]</sup> Specific modifications can be introduced by incorporating unnatural amino acids, site-specific mutations, or recombinant tags, but each method leads to a custom-designed antibody that is expensive to produce and significantly complicates the workflow.<sup>[32]</sup> Instead, an ABD carrying a desired chemical modification can be used to introduce a structurally well-defined modification to the antibody.<sup>[33–35]</sup> Since the Z domain binds at a hydrophobic patch between the constant domains 2 and 3 of the heavy chain (CH<sub>2</sub> and CH<sub>3</sub>), the binding of Z does not interfere with antigen binding.

A major drawback of using the existing ABDs for indirect antibody modification is that the resulting antibody complexes are short-lived due to limited affinity (in the range of low to high nanomolar at best) and the high rate of association and dissociation.<sup>[36]</sup> For example, bound Z dissociates within 5 min, meaning that any intended antibody modification would be lost on the same time scale.<sup>[37–39]</sup> The bound complex may be crosslinked by incorporating an unnatural amino acid with a photoactivatable side chain in ABD and exposing the complex to UV light.<sup>[39–43]</sup> It is challenging to produce a uniformly crosslinked complex because the efficiency of photocrosslinking is low and the complex can dissociate during UV treatment, although incomplete conjugation does not interfere with some applications, such as immunohistochemistry.<sup>[44]</sup> The additional steps needed to crosslink the complex also make it challenging to produce the reagent at scale.

In this study, we describe the construction of a novel antibody-binding protein with a significantly higher antibody affinity. We focus on affinity improvement because it allows the antibody-bound complex to remain bound during application without covalent crosslinking, thus making the molecule more convenient to use for introducing targeted antibody modification. Because the complex is stabilized through noncovalent interaction, there are no additional steps needed other than mixing the components. To increase the affinity of interaction, we joined two Z domains using a long linker (“L”) to allow simultaneous binding of both domains to the same antibody. The affinity of this molecule, ZLZ, was 10- to 12-fold higher than that of a single Z domain and similar to that of full-length SpA despite its significantly smaller size. A tandem Z dimer, ZZ, has been reported but previous studies did not optimize the linker length, resulting in only a modest increase in the binding affinity.

We further joined the amino and carboxyl termini of ZLZ to create a circularized peptide (“lasso”) that is compact and potentially more stable against proteolytic degradation than a linear molecule, which may be important for downstream applications. The lasso binds with  $K_D = 0.53$  nM and has a dissociation half-life of 5 h at 37 °C. The circularized lasso design is useful because it contains two conformationally flexible linkers that can be independently engineered to introduce new biochemical properties without affecting antibody binding. We demonstrate these design features by constructing a lasso containing PRS in order to report the activity of a protease based on measured fluorescence. The high antibody affinity of a lasso and its tolerance

to mutations in the linker sequence may be utilized to develop novel biotechnology applications.

## 2. Experimental Section

### 2.1. Plasmid Construction

#### 2.1.1. Bacterial Expression Vectors

All expression vectors were constructed by introducing the corresponding genes into pET32a, from which the thioredoxin gene has been removed. pET32-6His-AviTag-Z was constructed by PCR amplifying the Z sequence corresponding to the amino acids (-7)-58 (according to the amino acid numbering given in Jendeborg et al.,<sup>[37]</sup> Figure 2) and ligating it into the vector together with an N-terminal hexahistidine and AviTag and a C-terminal FLAG epitope. pET32-6His-AviTag-ZZ was cloned by inserting a second Z domain directly after the first Z domain. pET32-6His-AviTag-ZLZ was cloned by introducing additional glycine and serine residues between the two Z domains to increase the number of linker residues. To construct pET32-NpuC-6His-AviTag-ZLZ-NpuN, the second Z sequence of pET32-6His-AviTag-ZLZ was first removed using *EcoRI* and *XhoI*, and replaced with Z and NpuN in a three-piece ligation. The intermediate construct was then digested with *NdeI* and *SalI*, into which NpuC and 6His-AviTag were inserted into a three-piece ligation. The final lasso construct after all cloning contains the following elements: (*NdeI*)-NpuC-(*SpeI*)-6His-AviTag-(*SalI*)-Z-(*EcoRI*)-L-Z-(*NheI*)-NpuN-(*XhoI*), where the restriction enzymes used for the cloning are indicated in parentheses. The sequences of all proteins used in the study are shown in Figures S1 and S4, Supporting Information.

#### 2.1.2. Yeast Display Vector

pCT302<sup>[45]</sup> was used to express human immunoglobulin G1 (IgG1) Fc fragment (hFc). The DNA fragment encoding the amino acids of the hFc fragment was amplified from pVitr01-trastuzumab (TZ; Addgene Plasmid #61883). The PCR product was digested and ligated into pCT302 using *NheI* and *BamHI* to place hFc at the C-terminus of Aga2. The mouse IgG1 Fc fragment (mFc) sequence was amplified from S14-Jamc.2 (Addgene Plasmid #28216) and similarly cloned into pCT302 for yeast surface display.

## 2.2. Protein Expression and Purification

### 2.2.1. Induction of Expression

BL21 (DE3) pLysS cells were transformed with various expression vectors and plated on LB agar (Boston BioProducts) containing 100 µg mL<sup>-1</sup> ampicillin. Several colonies were picked from the plate to initiate an overnight culture, which was diluted 100-fold into the induction medium composed of Terrific Broth (TB; Boston BioProducts) and 0.5% glycerol with 100 µg mL<sup>-1</sup> ampicillin. The cells were grown at 30 °C and 300 rpm until OD<sub>600</sub> = 0.4, and isopropyl β-D-1-thiogalactopyranoside was added to the final

concentration of 100  $\mu\text{M}$ . The cells were then cultured at 20 °C and 300 rpm for 18 h.

In vivo biotinylation was achieved by coexpressing an AviTag containing protein and the bacterial biotin-protein ligase BirA. To prepare biotinylated Z, for example, BL21(DE3) pLysS cells were cotransformed with pET32-6His-AviTag-Z and pET28-MBP-BirA and grown on LB agar containing 100  $\mu\text{g mL}^{-1}$  ampicillin and 50  $\mu\text{g mL}^{-1}$  kanamycin. The induction medium was the same as before, except that it now contained 300  $\mu\text{M}$  biotin. Biotinylation was tested by incubating purified protein with streptavidin and analyzing the complex by sodium dodecyl sulfate-polyacrylamide gel electrophoresis (SDS-PAGE). A change in electrophoretic mobility caused by streptavidin binding was used to confirm successful biotinylation of the molecule.

### 2.2.2. Affinity and Ion-Exchange Chromatography

Cells were harvested by centrifugation and lysed with B-per (Thermo Fisher Scientific). The cell lysate was centrifuged at 12 000 rpm for 10 min to isolate the soluble fraction. Twenty millimolar imidazole was added to the supernatant and the pH was adjusted to 7.5 with NaOH. PMSF (ACROS Organics) was added to 1 mM. The sample was filtered through a 0.2  $\mu\text{m}$  filter (Corning) and mixed with Ni-NTA resin that was pre-equilibrated in the wash buffer (WB), which is phosphate-buffered saline (PBS) supplemented with 500 mM NaCl, 1 mM PMSF, and 1% Triton X-100 (Sigma-Aldrich). The mixture was rocked at 4 °C for 30 min and poured into an empty column (BioRad). The flow-through was collected and poured over the same column three times. The column was washed with five column volumes of WB, and the bound protein was eluted with 100 mM imidazole in PBS. Five millimolar dithiothreitol (DTT) was added to the lasso eluate immediately to prevent oxidation of the cysteine side chain. The yield was estimated based on  $A_{280}$  measurement and visualized by Coomassie Blue (ThermoFisher Scientific) staining after SDS-PAGE. The eluate was buffer exchanged to 20 mM phosphate buffer (pH 7.5) and 1 mM PMSF and further purified by anion exchange chromatography using Mono Q 5/50 GL on the AKTApurifier plus workstation (GE Healthcare). After equilibration, the bound protein was eluted using a linear NaCl gradient from 120 to 320 mM NaCl over 30 mL. The fractions containing the lasso were combined and concentrated. Approximately 6–10 mg of purified biotinylated lasso was obtained from 1 L of cell culture.

### 2.3. Fluorescein Isothiocyanate (FITC) Conjugation of lasso

To introduce a site-specific modification at the cysteine side chain, the lasso was buffer-exchanged into PBS without DTT. Twenty-fold excess of fluorescein-5-maleimide (ThermoFisher Scientific) in dimethyl sulfoxide was added and allowed to react for 1 h at 20 °C. The reaction was quenched by adding 10 mM DTT. Excess reagent was removed by ultrafiltration, and the modified lasso was buffer-exchanged to PBS. FITC conjugation was visualized by running an SDS-PAGE gel and illuminating the gel with UV.

## 2.4. Yeast Display and Flow Cytometry

### 2.4.1. Induction and Labeling

The *Saccharomyces cerevisiae* strain EBY100 was transformed with pCT302-hFc or pCT302-mFc and selected on a SD-CAA plate lacking Trp and Ura. SD-CAA drop-out medium was inoculated with four to six colonies from the plate and grown overnight to  $\text{OD}_{600} = 4\text{--}5$ . The hFc/mFc expression was induced by switching the medium to SG-CAA, containing galactose, and growing the cells for 20 h at 30 °C. The expression of hFc/mFc was checked by labeling  $5 \times 10^5$  cells with M2 antibody (Agilent Technologies) against the C-terminal FLAG epitope. Fluorescence was analyzed by flow cytometry using BD LSRFortessa (Becton Dickinson). To test the binding of various antibody-binding proteins, hFc/mFc-displaying yeast cells were labeled with biotinylated Z, ZZ, ZLZ or the lasso at 20 °C for 30 min, washed in PBS and then incubated with streptavidin–phycoerythrin (SAPE) on ice for 30 min before flow cytometric analysis.

### 2.4.2. Affinity Measurement

To measure the affinity of binding, yeast cells were labeled with different concentrations of each antibody-binding protein (Z, ZZ, ZLZ, or lasso). The mean fluorescence intensity (MFI) of the displaying population was computed by subtracting the weighted background MFI from the total MFI<sup>[46]</sup> and was fit to a binding curve using the maximum MFI and the binding constant  $K_D$  as two fitting parameters.<sup>[46]</sup> Each measurement was repeated three times and fit three times. The average and the standard deviation of the mean were computed from measured  $K_D$  values.

### 2.4.3. Measurement of $k_{\text{off}}$ by Yeast Display

Yeast cells ( $4 \times 10^5$ ) displaying hFc were washed in PBS (pH 7.5) and incubated with 100 nM lasso for 30 min at room temperature. The cells were washed twice and resuspended in 5 mL PBS in a 15 mL conical tube. The tube was rocked gently at 37 °C for 2 h, washed, and resuspended in 5 mL PBS. The 2 h wash was repeated, and the cells were again resuspended in 5 mL PBS to start the dissociation phase of the measurement. While keeping the cells with bound lasso at 37 °C under constant, gentle rocking, 500  $\mu\text{L}$  of cells were taken at 1 h, 2 h, 3 h, and 4 h, washed, and labeled for 15 min with 0.1  $\mu\text{L}$  of SAPE on ice. The fluorescence intensity of the cells was measured by flow cytometry and fit to an exponential curve to compute the dissociation rate.

### 2.5. Affinity Measurement by ELISA

Streptavidin was adsorbed on a Nunc MaxiSorp flat-bottom 96-well plate. After washing in PBS-T (PBS with 0.05% Tween 20) and blocking with PBS-T containing 1% BSA, biotinylated lasso was added at a concentration of 0.25 or 5  $\mu\text{g mL}^{-1}$ . Serially diluted TZ (human anti-HER2 IgG1, TZ) was added across the plate in triplicates and incubated for 1 h at room temperature. Bound TZ

was detected with anti-human IgG-HRP using 3,3',5,5'-tetramethylbenzidine (TMB) as a substrate (Thermo Fisher Scientific). The absorption at 450 nm was measured on a FilterMax F5 96-well plate reader (Molecular Devices). Alternatively, 1  $\mu\text{g mL}^{-1}$  recombinant HER2 (Sino Biological) was immobilized on a Nunc MaxiSorp flat-bottom 96-well plate. The plate was washed in PBS-T and then blocked with PBS-T containing 1% BSA. TZ (5  $\mu\text{g mL}^{-1}$ ) was added to detect HER2, and serially diluted biotinylated lasso was added across the wells in triplicates for 1 h at room temperature. Avidin-HRP (Thermo Fisher Scientific) was added in 1:250 dilution for 0.5 h, and TMB was used as a substrate for reporting. The affinity of binding was measured by fitting the measured  $A_{450}$  to a binding curve:

$$f = f_0 \times \frac{[\text{lasso}]}{[\text{lasso}] + K_D}$$

with  $f_0$  and  $K_D$  as two fitting parameters.

## 2.6. Confocal Microscopy

Mesenchymal stem cells (MSCs; 40 000 cells) were seeded in a Nunc 48-well glass-bottom plate (Thermo Fisher Scientific). The cells were washed in PBS and fixed in 4% PFA for 15 min at room temperature. The cells were washed again in PBS before being permeabilized with 0.1% Triton X-100 for 1 h. The cells were then rinsed in PBS and blocked with 1% BSA, after which rabbit anti-human  $\alpha$  smooth muscle actin ( $\alpha$ -SMA; Abcam) was added to some wells at a 1:50 dilution. The remaining wells did not receive  $\alpha$ -SMA and served as a negative control. After overnight incubation at 4 °C, 500 nm FITC-conjugated lasso was added to some wells for 1 h. 4',6-Diamidino-2-phenylindole (DAPI) nuclear

stain was added for 5 min before the cells were analyzed by confocal fluorescence microscopy.

## 2.7. Protease-Dependent Release of Bound Lasso

To develop a lasso that is susceptible to proteolysis by tobacco etch virus (TEV), two copies of the protease recognition sequence (PRS) of the TEV protease (ENLYFQ[S]) were introduced in the linker surrounding biotinylated AviTag and FITC-conjugated cysteine. A total of  $5 \times 10^5$  yeast cells displaying hFc were washed in buffer A (50 mM Tris, pH 7.5 at 20 °C, 150 mM NaCl, 1 mM  $\beta$ -mercaptoethanol) and labeled with 500 nm lasso (with or without tobacco etch virus protease recognition sequence [PRS<sub>TEV</sub>]) for 1 h at room temperature. The cells were washed twice and resuspended in 250  $\mu\text{L}$  of the same buffer, which was then divided into five tubes of equal volume. Next, 0  $\mu\text{L}$ , 0.1  $\mu\text{L}$ , 0.2  $\mu\text{L}$ , 0.5  $\mu\text{L}$ , 1  $\mu\text{L}$ , or 2.5  $\mu\text{L}$  of TEV protease (MilliporeSigma) was added to the tubes to initiate proteolysis. The reaction was continued at 30 °C for 1 h before being quenched by placing the tubes on ice. The cells were washed in cold buffer A twice and resuspended in 50  $\mu\text{L}$  of the same buffer. SAPE (0.1  $\mu\text{L}$ ) was added for 15 min on ice, and the cells were washed twice before analysis by flow cytometry.

## 3. Results

### 3.1. Connecting Z Domains with a Flexible Linker Significantly Increases Antibody Affinity

The Z domain binds a subset of antibodies at the CH<sub>2</sub>–CH<sub>3</sub> interface of Fc with high affinity. To increase the binding affinity through multivalent interaction,<sup>[47]</sup> we joined two

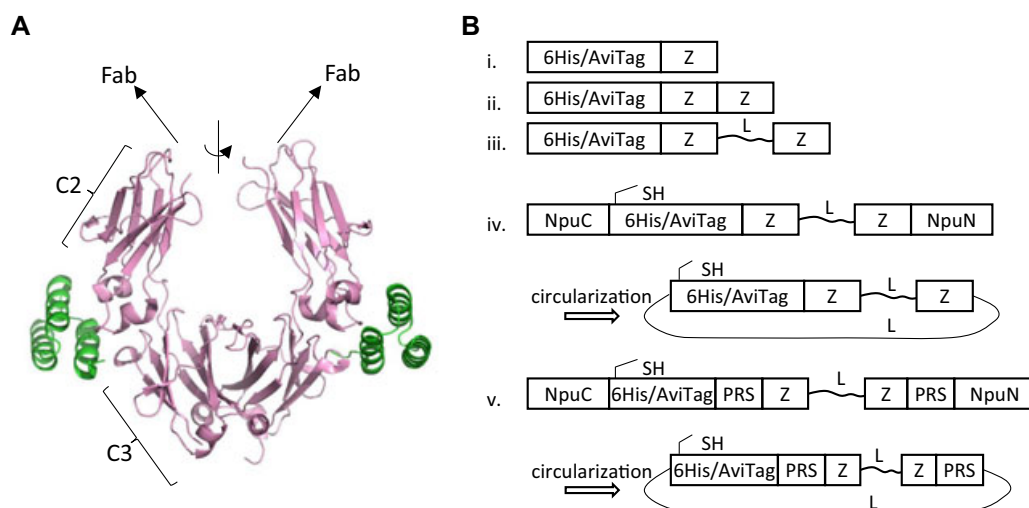


**Figure 1.** Schematics of the different antibody binding proteins used in this study. A) Antibody Fc (pink) with two Z domains (green) bound to the region between the C2 and C3 domains of Fc. The twofold symmetry axis is indicated with a line and a curved arrow. The location of the Fab fragment is indicated. B) Schematics of various antibody-binding proteins that were constructed and tested in the current study. AviTag is a 15-amino-acid biotin acceptor sequence, GLNDIFEAQKIEWHE, which is recognized by the biotin ligase, BirA. L (linker) refers to a set of conformationally flexible amino acids between Z domains. After circularization, the resulting lasso has two such linkers. NpuN and NpuC are the N and C fragments of the *Npu* DnaE split intein. The first amino acid after NpuC is cysteine, whose thiol side chain is shown.



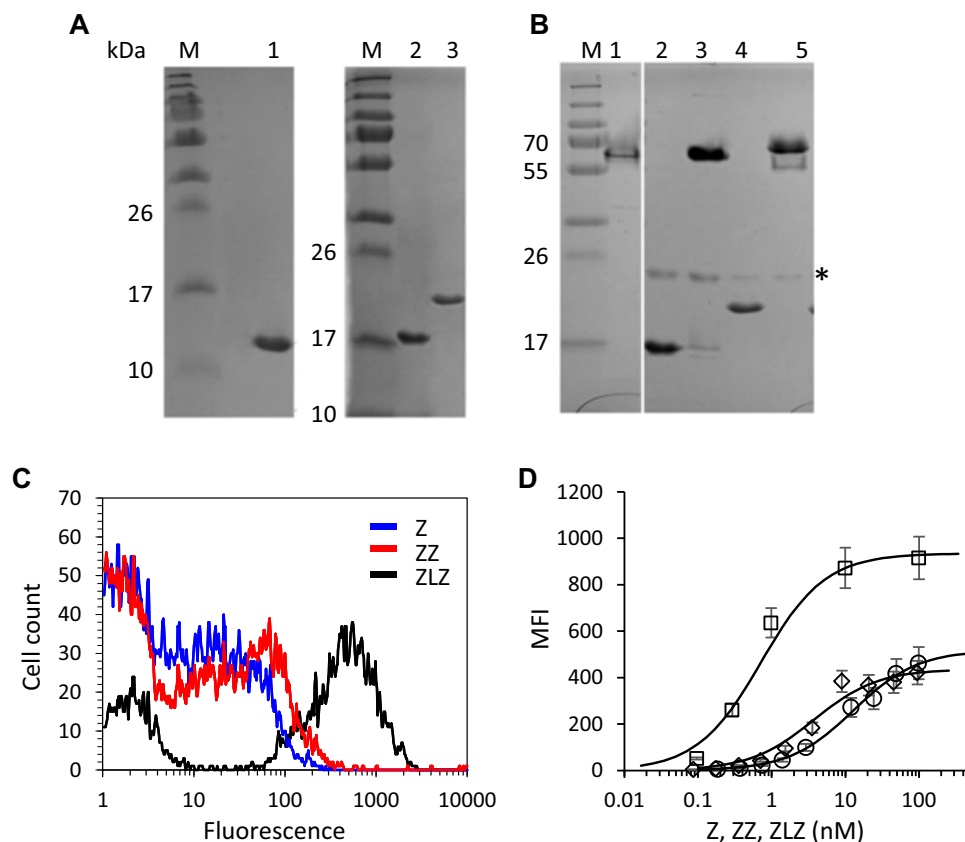


**Figure 2.** Improved antibody binding by a bivalent Z dimer. A) SDS-PAGE of purified 1, Z; 2, ZZ; and 3, ZLZ with the predicted molecular weights of 11 kDa, 17.7 kDa, and 19.0 kDa. M, protein molecular weight marker. B) In vivo biotinylation of ZZ and ZLZ was tested by EMSA by addition of streptavidin (SA). The binding of SA changes the mobility of a biotinylated ligand. 1, SA; 2, ZZ; 3, ZZ + SA; 4, ZLZ; and 5, ZLZ + SA. \* Indicates an unrelated bacterial protein present in this particular prep. C) yeast displayed hFc was labeled with biotinylated Z, ZZ, or ZLZ (each at 1 nM) and visualized with SAPE. D) Yeast cells were labeled with serially diluted biotinylated Z (circle), ZZ (diamond), or ZLZ (square) to measure the binding affinity. The cells were labeled, washed, and analyzed independently three times to obtain three  $K_D$  values, which were then used to compute the average and standard deviation presented in Table 1. Each data point on the graph represents the mean and standard deviation of the fluorescence measured at the indicated protein concentration.

Z domains through a conformationally flexible linker “L” to allow simultaneous binding of both Z domains to the same antibody (Figure 1A). The length of the linker was guided in part by molecular modeling and in part by a previous study, which suggested that a linker of 30 amino acids (DDAKK)<sub>6</sub> was able to connect two proteins bound to the CH<sub>2</sub>-CH<sub>3</sub> interfaces.<sup>[33]</sup> Including structurally disordered residues of bound Z (PDB 5U4Y), we estimate that there are 32 disordered amino acids in the linker, which are expected to be long enough to bridge two bound Z molecules. ZLZ differs from a tandem ZZ dimer,<sup>[48]</sup> which does not allow cooperative binding on the same antibody (Figure 1B; Figure S1, Supporting Information). To test the design, we purified Z, ZZ, and ZLZ from bacteria (Figure 2A). Each construct contains an AviTag,<sup>[49]</sup> which is biotinylated in vivo by coexpressing BirA in the same cell during expression.<sup>[50]</sup> We confirmed the biotinylation of the molecules using electrophoretic mobility shift assay (EMSA, Figure 2B).

Purified Z, ZZ, and ZLZ were used to label human IgG1 displayed on the yeast surface.<sup>[51]</sup> Bound protein was detected with SAPE and measured by flow cytometry (Figure 2C). We

then measured the binding affinity by titrating the concentration of each molecule and fitting the fluorescence of the displaying population to a binding curve (Figure 2D; Figure S2, Supporting Information). The affinity values measured using yeast display and flow cytometry are usually similar to the values obtained by SPR.<sup>[46,52]</sup> The affinity of ZZ ( $K_D = 5.5$  nM) was twofold higher than that of Z ( $K_D = 9.6$  nM), and both estimates were consistent with previously reported values in the literature (Table 1). Interestingly, the affinity of ZLZ was significantly higher than both,  $K_D = 0.72$  nM. A variant of ZLZ containing a linker with five fewer amino acids, ZL<sub>27</sub>Z, bound significantly less efficiently than ZLZ at the same concentration (Figure S3, Supporting Information), suggesting that a longer linker contributes to the higher affinity of ZLZ.

### 3.2. Circularized ZLZ Retains High-Binding Affinity

Because long linear ZLZ can bind and crosslink multiple antibodies, we circularized ZLZ by fusing the N and C fragments of *Npu* DnaE split intein to the carboxy and amino

**Table 1.** Summary of biochemical measurements.

Binder	MW [kDa]	$K_D$ [nM]	$k_{off}$ [s <sup>-1</sup> ]	References
Z		10–20	$2.1\text{--}3.2 \times 10^{-3}$	Jendeborg et al., Braisted et al., and Konrad et al. <sup>[37–39]</sup>
	11.0	$9.6 \pm 1.5$	NA	This work (flow cytometry)
		$12.1 \pm 1.0$	NA	This work (ELISA)
ZZ		1.5	$5.6 \times 10^{-4}$	Jendeborg et al. <sup>[37]</sup>
	17.7	$5.5 \pm 1.1$	NA	This work (flow cytometry)
		$5.0 \pm 0.9$	NA	This work (ELISA)
ZLZ	19.0	$0.72 \pm 0.23$	NA	This work
Lasso	19.5	$0.53 \pm 0.17$	$9.1 \times 10^{-5}$ at 37 °C	This work (flow cytometry)
			$1.7 \times 10^{-5}$ at 20 °C	
		$1.8 \pm 0.2$	$3.7 \times 10^{-5}$ at 37 °C	This work (ELISA)
		$0.79 \pm 0.2$	$3.8 \times 10^{-5}$ at 37 °C	This work (SPR)

The molecular weight (MW) represents the construct used in the current study, including 6xHis affinity tag, AviTag, and linkers. The mean and the standard deviation of three independent measurements are shown.

termini of the molecule, respectively (Figure 3A; Figure S4A, Supporting Information).<sup>[53,54]</sup> One way the circularized peptide can bind an antibody is by forming a circle around the Fc fragment, for which reason we named the molecule “antibody lasso.” The lasso contains an AviTag for in vivo biotinylation. The lasso was purified to homogeneity by a combination of hexahistidine affinity purification and ion exchange chromatography (Figure S4B, Supporting Information). We confirmed the successful biotinylation of the lasso by performing EMSA with streptavidin (Figure 3B). The lasso had an apparent molecular weight (MW) of  $\approx 17$  kDa on the gel, which is less than the computed MW of 19 766 Da. However, circularization sometimes increases the mobility of a protein, potentially by removing charged termini.<sup>[55]</sup> To confirm the formation of a circularized peptide, we measured the MW of purified lasso by MALDI-TOF (University at Albany, Proteomics/Mass Spectrometry Facility). The measured MW of 19 766 Da agrees exactly with the predicted MW of a circularized lasso containing a single biotin group (Figure S4C, Supporting Information).

### 3.3. Lasso Can Be Enzymatically or Chemically Modified to Introduce Novel Functions

We tested the binding of purified lasso to yeast displaying human and mouse Fc. Bound lasso was labeled with SAPE and analyzed. The yeast-displayed hFc were selectively labeled (Figure 3C). No labeling of yeast-displayed mFc was detected. The *Npu* DnaE-mediated splicing introduces a cysteine residue at the splice junction. We used maleimide-FITC to conjugate a fluorescent dye to the lasso,<sup>[56]</sup> thus producing a lasso containing two modifications, i.e., a biotin tag and a chemically conjugated fluorophore. The successful FITC conjugation was visualized on a native polyacrylamide gel by exposing the gel to UV (Figure 3D). To test for dual modification, we labeled hFc

displaying yeast cells with the lasso and further labeled them with SAPE. The displaying cells were both FITC- and PE-positive (Figure 3E), showing that a modification at the cysteine residue does not interfere with antibody binding or streptavidin detection. The yeast-displayed hFc was efficiently labeled even when the lasso was added at a concentration well below 1 nM, indicating a high affinity of interaction (Figure 3F). We measured the affinity by titrating the lasso concentration and fitting the measured fluorescence to a binding curve.<sup>[46]</sup> The measured affinity of binding  $K_D$  is 0.53 nM, which is similar to that of linear ZLZ and 10- to 20-fold higher than that of Z or ZZ (Figure 3G). Therefore, circularization of the lasso does not prevent high-affinity antibody binding achieved by rational design of the linker.

### 3.4. Lasso Produces Stronger ELISA Signals than Secondary Antibody

The binding of lasso to full-length human antibody, TZ, in solution was measured by SPR, which confirmed the measurement by flow cytometry. The measured rate of dissociation was  $3.8 \times 10^{-5} \text{ s}^{-1}$  at 37 °C, which is 55- to 84-fold slower than that for Z (Figure S5, Supporting Information). To test the use of lasso in ELISA, we immobilized biotinylated lasso on a streptavidin-coated surface and used it to capture TZ. The bound TZ was then detected using an HRP-conjugated anti-human antibody (Figure 4A). The binding of TZ was dependent on the lasso concentration and saturable, indicating that the binding is specific. Next, we physically adsorbed HER2 on the surface and used it to capture TZ, which was then detected with Z, ZZ, or lasso. The ligand concentration was varied to measure the binding constant  $K_D$ , which was the lowest for the lasso (Figure 4B). The measured  $K_D$  was consistent with the estimates from yeast display and SPR, as well as published results in the literature (Figures 2D, 3G, and Table 1). Finally, we compared the efficiency of immobilized biotinylated lasso or immobilized secondary antibody Fab fragment for capturing titrated TZ. The measurements at the four lowest concentrations were fit to a straight line and extrapolated to the lowest TZ concentration at which the measured signal is statistically indistinguishable from the mean blank signal ( $0.05 \pm 0.01$ ). The computed limit of detection (LOD) was  $0.13 \text{ ng mL}^{-1}$  for the lasso and  $1.6 \text{ ng mL}^{-1}$  for the adsorbed anti-human Fab antibody (aHuFab) fragment (Figure 4C), suggesting that the lasso was able to capture antibody with improved sensitivity.

### 3.5. A Lasso-Based Sensor Can Detect Protease Activity

Because the linker residues are not expected to interact specifically with antibody residues, we reasoned that they may be mutated without affecting antibody binding. We incorporated two copies of the PRS<sub>TEV</sub> in one of the linkers, thus making the lasso susceptible to proteolysis by a protease (Figure 5A; Figure S4D, Supporting Information). The lasso containing PRS<sub>TEV</sub> bound immobilized TZ with the same affinity as before (Figure 5B). Proteolysis by TEV protease cuts

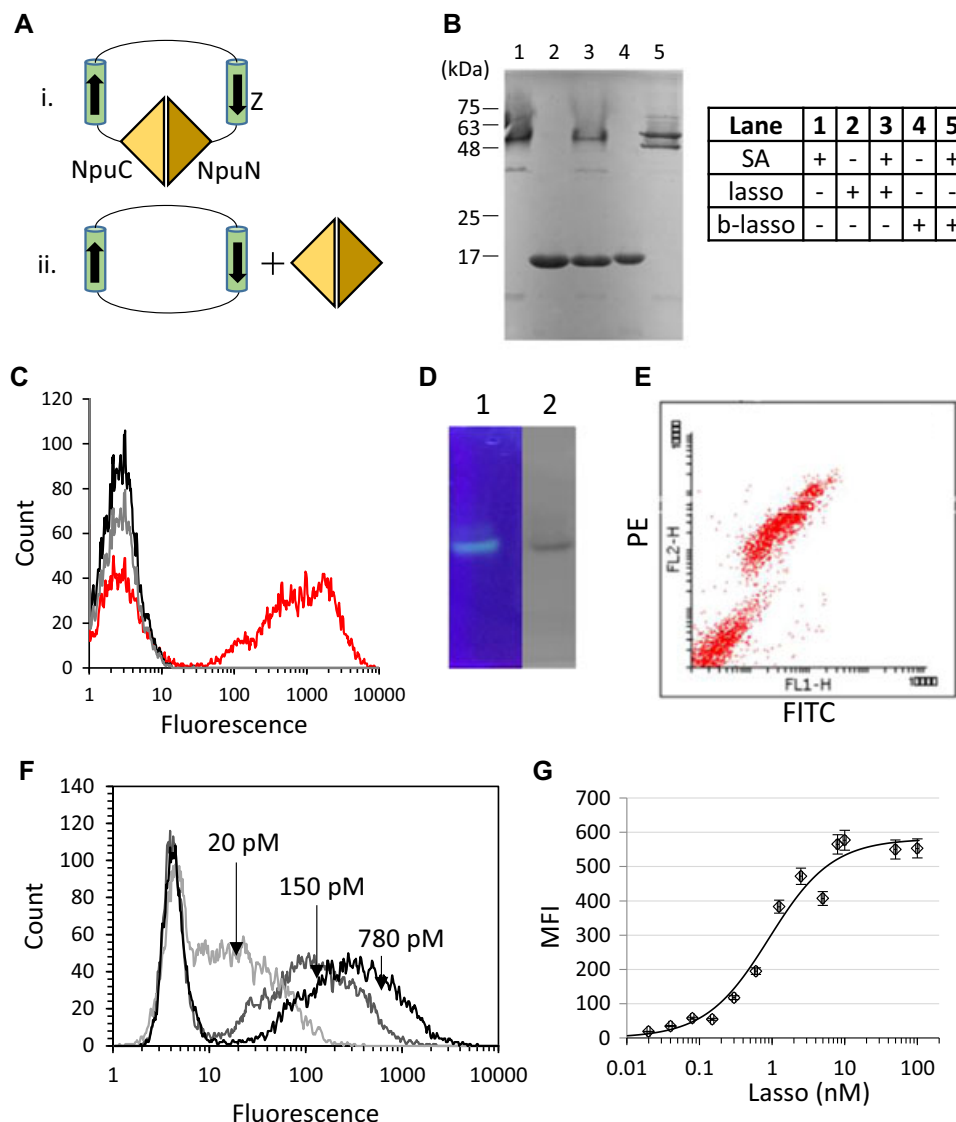


**Figure 3.** Construction and characterization of a circularized antibody-binding protein. A) Schematic description for constructing a circularized antibody-binding lasso. i) The precursor to the lasso contains NpuC at the amino terminus and NpuN at the carboxy terminus. ii) The split intein domains reconstitute the splicing activity and join the neighboring amino acids in a native peptide bond while excising themselves out. B) Checking the biotinylation of lasso by EMSA. The binding of SA is specific and occurs with biotinylated lasso (b-lasso) only. C) Yeast-displayed hFc (red) or mFc (gray) was labeled with biotinylated lasso and SAPE and analyzed by flow cytometry. Untransformed yeast was similarly labeled for comparison (black). D) Lasso was conjugated with maleimide-FITC and analyzed by native polyacrylamide gel electrophoresis. 1) UV illumination of the gel. 2) Coomassie staining of the same gel. E) Yeast-displayed hFc was labeled with biotinylated FITC-conjugated lasso and SAPE, and analyzed by flow cytometry. F) Yeast-displayed hFc was labeled with 20 pM, 150 pM, or 780 pM of biotinylated lasso to show efficient labeling at sub-nanomolar concentrations. G) The lasso concentration was titrated and the MFI of displaying population was used to compute the binding constant,  $K_D = 0.53 \text{ nM} \pm 0.17 \text{ nM}$  (mean and the standard deviation of the mean,  $n = 3$ ).

the lasso into two linear peptides, one of which contains no Z domain and is released from the antibody. We labeled yeast-displayed hFc with the new lasso and measured the fluorescence of the cells after adding TEV protease. The fluorescence decreased with an increasing concentration of TEV protease, indicating loss of the FITC-conjugated peptide (Figure 5B). In contrast, the fluorescence of the cells labeled with the original lasso without PRS<sub>TEV</sub> remained constant when TEV protease was added (Figure 5B).

### 3.6. FITC-Conjugated Lasso Can Detect Cell-Bound Antibody for Fluorescence Microscopy

Since the lasso binds full-length antibody with high affinity, it may be used to introduce a noncovalent modification to the antibody for labeling applications. We cultured MSCs on glass slides, which were then fixed and permeabilized in preparation for fluorescence labeling. A rabbit anti- $\alpha$ -SMA antibody was added to bind the actin filaments and the bound antibody was

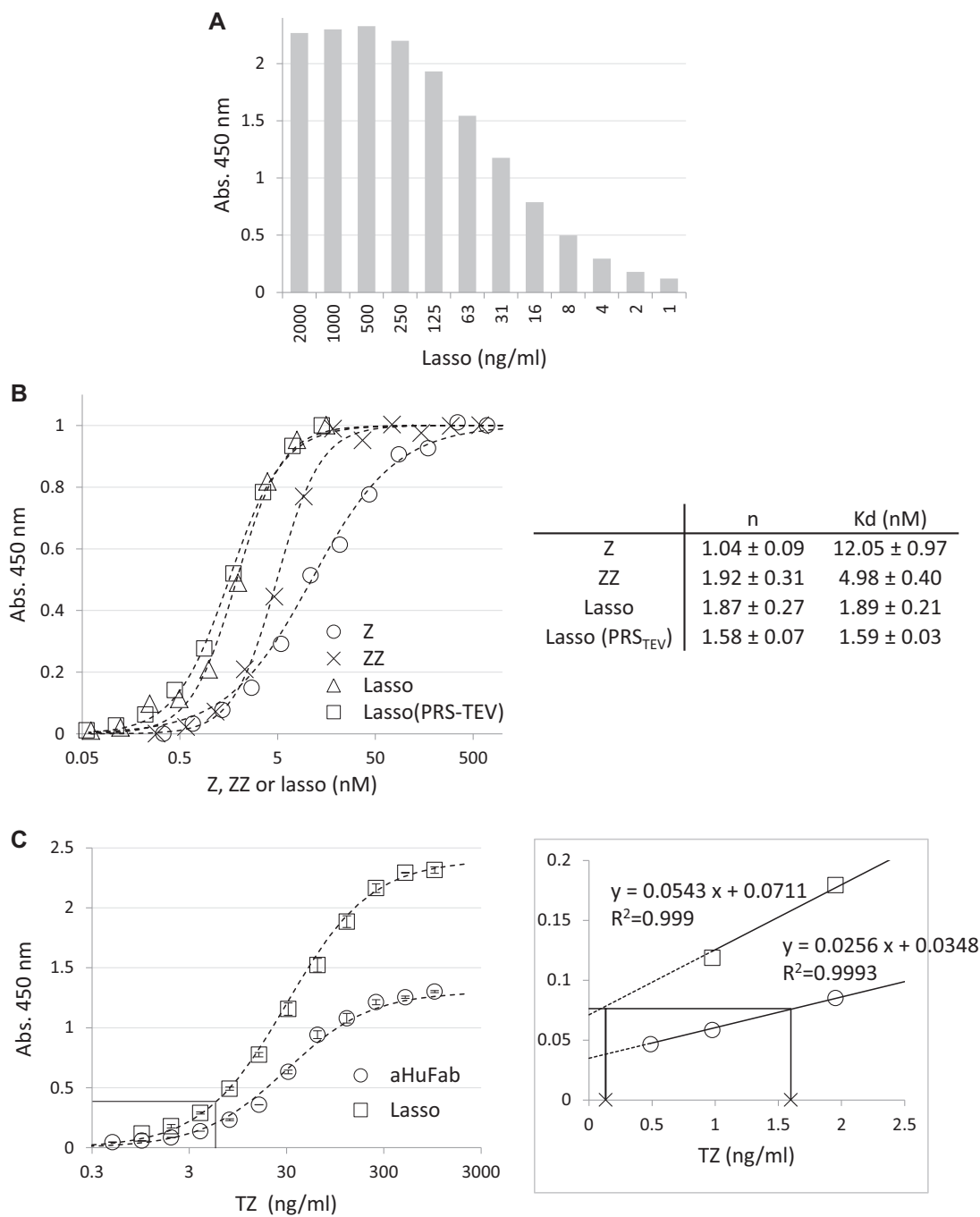


**Figure 4.** Improved sensitivity of ELISA detection using lasso. A) Biotinylated lasso was immobilized on a streptavidin-coated surface and used to capture TZ. The lasso concentration was titrated to vary the loading density, resulting in a more efficient capture of TZ. The captured TZ was detected using anti-human antibody-HRP conjugate. B) The equilibrium binding affinity of Z, ZZ, and two different variants of the lasso were measured by titrating each molecule to detect immobilized TZ. The normalized absorbance at 450 nm was fit to the equation  $A_{450} = \frac{[C]^n}{[C]^n + K_D^n}$ , where  $[C]$  is the concentration of Z, ZZ, or the lasso, to compute the binding constant  $K_D$  and the Hill coefficient  $n$ . The average and standard deviation from three separate measurements are shown. C) (Left) TZ was captured with immobilized lasso or the Fab fragment of aHuFab to compare the sensitivity of detection. Bound TZ was detected with an anti-human antibody. (Right) An enlarged view of the binding data from lower TZ concentrations. The four data points corresponding to the lowest TZ concentrations were used to generate a linear fit and to compute the LOD ( $\leftarrow$ ) for the two methods. The computed LOD are  $1.6 \text{ ng mL}^{-1}$  for aHuFab and  $0.13 \text{ ng mL}^{-1}$  for the lasso.



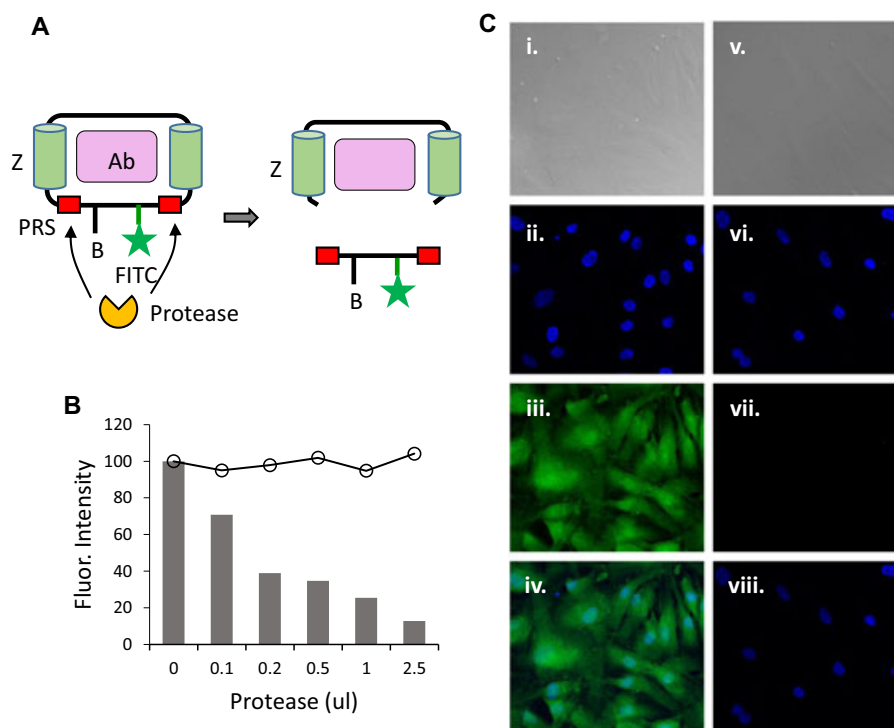


**Figure 5.** Potential applications of lasso in biotechnology. A) A lasso containing the PRS (red) for TEV protease. Two copies of PRS<sub>TEV</sub> surround the biotinylated AviTag (B) and FITC-conjugated cysteine. Proteolysis by TEV protease splits an antibody-bound lasso into two, one of which lacks a Z domain and is thereby dissociated from the antibody. B) Yeast-displayed hFc was labeled with the lasso containing PRS<sub>TEV</sub>, and TEV protease was added at different concentrations. There is a concentration-dependent loss of FITC fluorescence, indicating proteolysis by the protease (bar). On the other hand, TEV protease did not reduce the fluorescence from the original lasso without PRS<sub>TEV</sub> (circle), showing that the loss of fluorescence is due to sequence-specific proteolysis. Representative results from two independent measurements are shown. C) Fluorescent labeling of MSC with lasso. Fixed and permeabilized cells were treated with anti- $\alpha$ -SMA antibody (i–iv) or without antibody (v–viii). FITC-conjugated lasso and DAPI were then added to both. i, v) DIC; (ii, vi) DAPI; (iii, vii) FITC; (iv, viii) overlay of DAPI and FITC.

detected with FITC-conjugated lasso for visualization by confocal microscopy. A rabbit antibody was used since it is recognized by SpA with high affinity. The cells were labeled efficiently with FITC-lasso (Figure 5C). The cells labeled with lasso alone without the antibody were not fluorescent, indicating that the labeling was antibody-specific (Figure 5C, viii).

## 4. Discussion

### 4.1. Lasso Can Be Used to Form a Stable Antibody Complex

The existing methods for introducing site-specific modifications in antibodies are inconvenient, costly, and difficult to scale. Introducing a modification indirectly through an antibody-binding protein can simplify the task if the affinity of interaction can be improved. Here, we demonstrated that joining two bound Z domains with a long linker, as in ZLZ or lasso, increases the affinity of interaction by 13- to 18-fold compared to a single Z domain. Although the current study does not systematically screen the linker length, observations both by us and others indicate that the affinity of an interaction can be greatly improved by optimizing multivalent binding. For example, Dong et al.<sup>[33]</sup> reported that fusing the D domain of protein A and C1 domain of protein G with a 30 residue linker, (DDAKK)<sub>6</sub>, increases the binding affinity by 8.4- to 12-fold over

the individual domains. The same authors have noted that joining the domains with a shorter 20-amino-acid linker improves the binding affinity by only 2.9- to 4.2-fold, which is consistent with our observation that a linker of 27 amino acids may already be too short to bridge two bound Z proteins. The affinity for ZZ, which does not contain such a linker, is only approximately twofold higher. The improvement in binding affinity occurs mostly through slowing of the rate of dissociation, which is a direct consequence of multivalent interaction. These studies thus show that the apparent binding affinity of an interaction can be rationally improved by joining independently binding domains.<sup>[57]</sup>

### 4.2. A Bound Lasso May Adopt Many Alternative Conformations

One of the linkers in the engineered lassos (Linker1) is 32-amino-acids long, which is just long enough to connect the carboxy terminus of one bound Z domain with the amino terminus of another Z domain bound to the same antibody located  $\geq 70$  Å away. Because the second linker (Linker2) of the lasso is significantly longer (56–65 amino acids), it may sample many alternative conformations not available to Linker1. For example, it may swing from one side of Fc to the other (by hopping over the carboxy end of Fc) while both

Z domains remain bound to the antibody. The bound lasso is thus expected to adopt a range of conformations that vary in the positioning of Linker2 with respect to the antibody. To test the role of the second linker length, we constructed another lasso with 36 amino acids in both Linker1 and Linker2. The affinity of the modified lasso was significantly lower (and comparable to that of a single Z domain), indicating that the binding of a lasso with a small diameter may be kinetically limited (data not shown). Therefore, designing a lasso with the highest antibody affinity, and favorable binding kinetics, benefits from including the shortest linker compatible with cooperative binding (i.e., Linker1) to improve the dissociation kinetics and a longer linker (Linker2) to optimize the association kinetics.

### 4.3. Our Lasso Design Is Unique

A circularized protein is more resistant to nonspecific proteolytic degradation, e.g., by an exopeptidase. This has previously motivated the engineering of a circularized minimal Z domain,  $Z_{\min}$ , containing two antibody binding helices.<sup>[58]</sup> Despite some conceptual similarities, our lasso and  $Z_{\min}$  are fundamentally different in that our lasso contains two Z domains that cooperatively bind to the two binding sites in order to slow the dissociation rate, whereas the most significant advance in  $Z_{\min}$  is the thermal stabilization of the molecule without a clear improvement in the binding kinetics. Furthermore, the use of a split intein to engineer a circularized molecule directly in bacteria is unique to our study and differs from the in vitro circularization of a chemically synthesized peptide used in the design of  $Z_{\min}$ .

### 4.4. Lasso Improves ELISA Signal Compared to the Standard Technique Based on Secondary Antibody

The use of a lasso ensures more homogeneous modification of the antibody since every antibody at equilibrium is expected to bind one lasso molecule. This may explain the higher ELISA signal from lasso labeling than from secondary antibody (Figure 4C). When an antibody is chemically biotinylated, the degree of modification cannot be controlled precisely, leading to a range of modification in the final product. Some of the molecules may carry no modification, which then reduces the final signal intensity. There may be additional signal loss during the detection and reporting phase of ELISA because of the low affinity of binding for secondary antibodies. The lasso has high antibody affinity and a half-life of 5 h at 37 °C (and 11 h at 20 °C), which ensures that the complex remains intact during the incubation and washing steps. Together, the combination of higher binding affinity and consistent labeling should help improve the performance of a lasso-bound antibody in biosensing applications. The ability to form a stable complex with an antibody while introducing precise modifications makes the lasso a useful adapter protein. The potential use of the molecule for in vivo detection and reporting will be investigated in future studies.

### 4.5. Linkers Allow Design Flexibility and May Be Used to Develop a Localized Protease Sensor

Mutating the linker residues does not affect antibody binding significantly. For example, the lassos with or without PRS<sub>TEV</sub> bind full-length human antibody with the same affinity (Figure 5A). Thus, novel functions can be engineered into a lasso by custom designing one or both of its linkers. A lasso can continue to bind an antibody after enzymatic or chemical modifications and thereby endow the antibody with a novel function. We showed this by constructing a lasso with a biotin tag that generates a stronger ELISA signal than enzyme-conjugated secondary antibodies. Chemical conjugation of the unique cysteine residue with a reporter molecule, e.g., fluorophore or DNA, may also be used to introduce a structurally and stoichiometrically well-defined modification to an antibody with fine-tuned biochemical properties. We also constructed a lasso containing PRS to develop an antibody that functions as a protease sensor. The efficient proteolysis of a PRS containing lasso indicates that the linker residues remain accessible to an external enzyme while the molecule remains bound to the antibody (Figure 5B). Many diseases are characterized by an increase in tissue-specific protease activity, and engineered antibodies with protease-dependent activity have been developed to measure localized disease-associated protease activity.<sup>[59,60]</sup> A lasso with optimized PRS may be similarly used to develop an antibody-based reporter of local protease activity, but without direct modification of the antibody.

Although a protease sensor may be developed using a linear molecule, circularization improves the robustness and versatility of the design. For example, a lasso containing PRS1 and PRS2, for two orthogonal proteases will lose the reporter signal only when the molecule is exposed to both proteases near the antibody. An antibody-bound lasso may thus be used to monitor localized protease activity. On the other hand, linear ZLZ containing PRS1 and PRS2 would easily dissociate from the antibody after the proteolysis by either enzyme so that the loss of reporter activity cannot be used to determine the activity of more than one protease.

### 4.6. Lasso Can Immobilize Antibody on a Surface for Biosensing Applications

Biosensing applications sometimes require surface immobilization of an antibody.<sup>[61,62]</sup> Immobilizing an antibody through a chemical linker can improve its ability to subsequently interact with a ligand in solution, compared to immobilization based on nonspecific hydrophobic absorption that may denature the antibody or mask the antigen-binding sites.<sup>[63]</sup> To this end, a commercially available streptavidin-coated surface can be treated with a biotinylated lasso to create a generic antibody-capturing surface. The lasso can then bind unlabeled antibodies for antigen capture or for affinity measurement by SPR. The antibody capture efficiency (based on LOD) is an order of magnitude higher than an immobilized secondary antibody, which is commonly used for label-free capture. The binding is

specific and the dissociation of bound antibody is minimal. Both intact and modified antibody fragments have been immobilized and successfully used on other surfaces.<sup>[64,65]</sup> The lasso may offer an alternative tool to achieve antibody immobilization to complement existing technologies.

#### 4.7. Conclusion

Our goal in this study is to improve the affinity of an antibody-binding protein by joining two Z domains through a flexible linker. The linker needs to be above a certain minimum length in order to support bivalent interaction, which appears to be around 30 amino acids. Circularization of the molecule with a split intein creates a compact molecule that maintains high antibody affinity. The lasso may be modified with a reporter before binding an antibody to generate a functionalized probe. The precise linker sequence may be changed without loss of affinity to implement other features. For example, PRSs may be introduced to develop a lasso-based protease sensor, which may be targeted in vivo with an antibody. To our knowledge, this is the first demonstration that an engineered adapter protein may be used to introduce a stable modification to an antibody without resorting to genetic modification of the antibody or chemical crosslinking of the complex. The improved antibody affinity and sequence flexibility of a lasso make it an attractive tool for use in biotechnology applications.

#### Supporting Information

Supporting Information is available from the Wiley Online Library or from the author.

#### Acknowledgements

This work was in part supported with a grant from the National Science Foundation to S.P. (CBET 1264051). The authors acknowledge Dr. Dhaval Shah (University at Buffalo) for the use of a ELISA system.

#### Conflict of Interest

The authors declare no conflict of interest.

#### Keywords

antibody-binding protein, antibody modification, circularization, protease sensor, Z domain

Received: October 19, 2018  
Revised: January 27, 2019  
Published online: April 15, 2019

- [1] M. Jain, N. Kamal, S. K. Batra, *Trends Biotechnol.* **2007**, 25, 307.
- [2] P. J. Kennedy, C. Oliveira, P. L. Granja, B. Sarmento, *Crit. Rev. Biotechnol.* **2018**, 38, 394.
- [3] E. V. Sidorin, T. F. Solov'eva, *Biochemistry (Mosc.)* **2011**, 76, 295.
- [4] W. Choe, T. A. Durgannavar, S. J. Chung, *Materials (Basel)* **2016**, 9.
- [5] B. Serhir, R. Higgins, B. Foiry, M. Jacques, *J. Gen. Microbiol.* **1993**, 139, 2953.
- [6] W. Kastern, E. Holst, E. Nielsen, U. Sjöbring, L. Björck, *Infect. Immun.* **1990**, 58, 1217.
- [7] M. Meehan, P. Owen, Y. Lynagh, C. Woods, *Microbiology* **2001**, 147, 3311.
- [8] M. J. Lewis, M. Meehan, P. Owen, J. M. Woof, *J. Biol. Chem.* **2008**, 283, 17615.
- [9] J. Deisenhofer, *Biochemistry* **1981**, 20, 2361.
- [10] E. H. Sasso, G. J. Silverman, M. Mannik, *J. Immunol.* **1991**, 147, 1877.
- [11] K. Kato, L. Y. Lian, I. L. Barsukov, J. P. Derrick, H. Kim, R. Tanaka, A. Yoshino, M. Shiraishi, I. Shimada, Y. Arata, G. Roberts, *Structure* **1995**, 3, 79.
- [12] L. Yang, M. E. Biswas, P. Chen, *Biophys. J.* **2003**, 84, 509.
- [13] M. Tsukamoto, H. Watanabe, A. Ooishi, S. Honda, *J. Biol. Eng.* **2014**, 8, 15.
- [14] H. Hjelm, K. Hjelm, J. Sjöquist, *FEBS Lett.* **1972**, 28, 73.
- [15] K. Bauer, P. M. Bayer, E. Deutsch, F. Gabl, *Clin. Chem.* **1980**, 26, 297.
- [16] K. Huse, H. J. Böhme, G. H. Scholz, *J. Biochem. Biophys. Methods* **2002**, 51, 217.
- [17] M. Eliasson, A. Olsson, E. Palmcrantz, K. Wiberg, M. Inganas, B. Guss, M. Lindberg, M. Uhlen, *J. Biol. Chem.* **1988**, 263, 4323.
- [18] S. Hober, K. Nord, M. Linhult, *J. Chromatogr. B Analyt. Technol. Biomed. Life. Sci.* **2007**, 848, 40.
- [19] S. B. Hari, H. Lau, V. I. Razinkov, S. Chen, R. F. Latypov, *Biochemistry* **2010**, 49, 9328.
- [20] A. R. Mazzer, X. Perraud, J. Halley, J. O'hara, D. G. Bracewell, *J. Chromatogr. A* **2015**, 1415, 83.
- [21] T. Moks, L. Abrahmsen, B. Nilsson, U. Hellman, J. Sjoquist, M. Uhlen, *Eur. J. Biochem.* **1986**, 156, 637.
- [22] I. Dahlborn, D. Agardh, T. Hansson, *Clin. Chim. Acta* **2008**, 395, 72.
- [23] A. Bakhmachuk, O. Gorbatiuk, A. Rachkov, B. Dons'koi, R. Khristosenko, I. Ushenin, V. Peshkova, A. Soldatkin, *Nanoscale Res. Lett.* **2017**, 12, 112.
- [24] J. J. Langone, C. Das, R. Mainwaring, W. T. Shearer, *Mol. Cell. Biochem.* **1985**, 65, 159.
- [25] B. Nilsson, T. Moks, B. Jansson, L. Abrahmsén, A. Elmlblad, E. Holmgren, C. Henrichson, T. A. Jones, M. Uhlén, *Protein Eng.* **1987**, 1, 107.
- [26] T. Porstmann, S. T. Kiessig, *J. Immunol. Methods* **1992**, 150, 5.
- [27] J. H. Lee, H. K. Choi, J. H. Chang, *J. Immunol. Methods* **2010**, 362, 38.
- [28] N. G. Welch, R. M. T. Madiona, T. B. Payten, C. D. Easton, L. Pontes-Braz, N. Brack, J. A. Scoble, B. W. Muir, P. J. Pigram, *Acta Biomater.* **2017**, 55, 172.
- [29] G. J. L. Bernardes, M. Steiner, I. Hartmann, D. Neri, G. Casi, *Nat. Protoc.* **2013**, 8, 2079.
- [30] C. D. Spicer, B. G. Davis, *Nat. Commun.* **2014**, 5, 4740.
- [31] J. R. Junutula, H. Raab, S. Clark, S. Bhakta, D. D. Leipold, S. Weir, Y. Chen, M. Simpson, S. P. Tsai, M. S. Dennis, Y. Lu, Y. G. Meng, C. Ng, J. Yang, C. C. Lee, E. Duenas, J. Gorrell, V. Katta, A. Kim, K. McDorman, K. Flagella, R. Venook, S. Ross, S. D. Spencer, W. Lee wong, H. B. Lowman, R. Vandlen, M. X. Sliwowski, R. H. Scheller, P. Polakis, W. Mallet, *Nat. Biotechnol.* **2008**, 26, 925.
- [32] J. Y. Axup, K. M. Bajjuri, M. Ritland, B. M. Hutchins, C. H. Kim, S. A. Kazane, R. Halder, J. S. Forsyth, A. F. Santidrian, K. Stafin, Y. Lu, H. Tran, A. J. Sellar, S. L. Biroc, A. Szydluk, J. K. Pinkstaff, F. Tian, S. C. Sinha, B. Felding-Habermann, V. V. Smider, P. G. Schultz, *Proc. Natl. Acad. Sci. U. S. A.* **2012**, 109, 16101.
- [33] J. Dong, T. Kojima, H. Ohashi, H. Ueda, *J. Biosci. Bioeng.* **2015**, 120, 504.
- [34] J. T. Sockolosky, S. Kivimäe, F. C. Szoka, *PLoS One* **2014**, 9, e102566.
- [35] J. Park, Y. Lee, B. J. Ko, T. H. Yoo, *Bioconjugate Chem.* **2018**.

- [36] K. Saha, F. Bender, E. Gizeli, *Anal. Chem.* **2003**, 75, 835.
- [37] L. Jendeborg, B. Persson, R. Andersson, R. Karlsson, M. Uhlén, B. Nilsson, *J. Mol. Recognit.* **1995**, 8, 270.
- [38] A. C. Braisted, J. A. Wells, *Proc. Natl. Acad. Sci. U.S.A.* **1996**, 93, 5688.
- [39] A. Konrad, A. Eriksson karlström, S. Hober, *Bioconjugate Chem.* **2011**, 22, 2395.
- [40] A. Perols, A. E. Karlström, *Bioconjugate Chem.* **2014**, 25, 481.
- [41] J. Z. Hui, A. Tsourkas, *Bioconjugate Chem.* **2014**, 25, 1709.
- [42] S. Kanje, S. Hober, *Biotechnol. J.* **2015**, 10, 564.
- [43] G. Dormán, G. D. Prestwich, *Trends Biotechnol.* **2000**, 18, 64.
- [44] S. Andersson, A. Konrad, N. Ashok, F. Pontén, S. Hober, A. Asplund, *J. Histochem. Cytochem.* **2013**, 61, 773.
- [45] K. Hong lim, I. Hwang, S. Park, *Biotechnol. Prog.* **2012**, 28, 276.
- [46] G. Chao, W. L. Lau, B. J. Hackel, S. L. Sazinsky, S. M. Lippow, K. D. Wittrup, *Nat. Protoc.* **2006**, 1, 755.
- [47] V. M. Krishnamurthy, L. A. Estroff, G. M. Whitesides *Multivalency in Ligand Design, Fragment-based Approaches in Drug Discovery*, Wiley-VCH Verlag GmbH & Co. KGaA, Weinheim **2006**, pp. 11–53.
- [48] G. Rigaut, A. Shevchenko, B. Rutz, M. Wilm, M. Mann, B. Séraphin, *Nat. Biotechnol.* **1999**, 17, 1030.
- [49] A. Tirat, F. Freuler, T. Stettler, L. M. Mayr, L. Leder, *Int. J. Biol. Macromol.* **2006**, 39, 66.
- [50] A. Chapman-Smith, J. E. Cronan Jr., *Trends Biochem. Sci.* **1999**, 24, 359.
- [51] H. J. Choi, Y. J. Kim, D. K. Choi, Y. S. Kim, *PLoS One* **2015**, 10, e0145349.
- [52] V. Salema, L. Á. Fernández, *Microb. Biotechnol.* **2017**, 10, 1468.
- [53] J. Zettler, V. Schütz, H. D. Mootz, *FEBS Lett.* **2009**, 583, 909.
- [54] Y. Li, *Biotechnol. Lett.* **2015**, 37, 2121.
- [55] H. Iwai, A. Plückthun, *FEBS Lett.* **1999**, 459, 166.
- [56] S. B. Gunnoo, A. Madder, *ChemBioChem* **2016**, 17, 529.
- [57] S. Koide, J. Huang, *Methods Enzymol.* **2013**, 523, 285.
- [58] P. Järver, C. Mikaelsson, A. E. Karlström, *J. Pept. Sci.* **2011**, 17, 463.
- [59] I. J. Chen, C. H. Chuang, Y. C. Hsieh, Y. C. Lu, W. W. Lin, C. C. Huang, T. C. Cheng, Y. A. Cheng, K. W. Cheng, Y. T. Wang, F. M. Chen, T. L. Cheng, S. C. Tzou, *Sci. Rep.* **2017**, 7, 11587.
- [60] K. R. Wong, E. Menendez, C. S. Craik, W. M. Kavanaugh, O. Vasiljeva, *Biochimie* **2016**, 122, 62.
- [61] J. Y. Jyoung, S. Hong, W. Lee, J. W. Choi, *Biosens. Bioelectron.* **2006**, 21, 2315.
- [62] N. Patel, M. C. Davies, M. Hartshorne, R. J. Heaton, C. J. Roberts, S. J. B. Tendler, P. M. Williams, *Langmuir* **1997**, 13, 6485.
- [63] A. Kausaite-Minkstiniene, A. Ramanaviciene, J. Kirlyte, A. Ramanavicius, *Anal. Chem.* **2010**, 82, 6401.
- [64] Z. Balevicius, A. Ramanaviciene, I. Baleviciute, A. Makaraviciute, L. Mikoliunaite, A. Ramanavicius, *Sens. Actuators B-Chem* **2011**, 160, 555.
- [65] A. Makaraviciute, T. Ruzgas, A. Ramanavicius, A. Ramanaviciene, *Anal. Methods* **2014**, 6, 2134.